

Article

Comparative Production of Bio-Oil from In Situ Catalytic Upgrading of Fast Pyrolysis of Lignocellulosic Biomass

Ali Abdulkhani ¹, Zahra Echresh Zadeh ², Solomon Gajere Bawa ², Fubao Sun ³, Meysam Madadi ³, Xueming Zhang ⁴ and Basudeb Saha ^{5,*}

¹ Department of Wood and Paper Sciences and Technology, Faculty of Natural Resources, University of Tehran, Karaj 1417466191, Iran

² Department of Chemical Engineering, University College London, Torrington Place, London WC1E 7JE, UK

³ Key Laboratory of Industrial Biotechnology, Ministry of Education, School of Biotechnology, Jiangnan University, Wuxi 214122, China

⁴ Beijing Key Laboratory of Lignocellulosic Chemistry, College of Materials Science and Technology, Beijing Forestry University, Beijing 100083, China

⁵ School of Engineering, Lancaster University, Lancaster LA1 4YW, UK

* Correspondence: b.saha@lancaster.ac.uk

Abstract: Catalytic upgrading of fast pyrolysis bio-oil from two different types of lignocellulosic biomass was conducted using an H-ZSM-5 catalyst at different temperatures. A fixed-bed pyrolysis reactor has been used to perform in situ catalytic pyrolysis experiments at temperatures of 673, 773, and 873 K, where the catalyst (H-ZSM-5) has been mixed with wood chips or lignin, and the pyrolysis and upgrading processes have been performed simultaneously. The fractionation method has been employed to determine the chemical composition of bio-oil samples after catalytic pyrolysis experiments by gas chromatography with mass spectroscopy (GCMS). Other characterization techniques, e.g., water content, viscosity, elemental analysis, pH, and bomb calorimetry have been used, and the obtained results have been compared with the non-catalytic pyrolysis method. The highest bio-oil yield has been reported for bio-oil obtained from softwood at 873 K for both non-catalytic and catalytic bio-oil samples. The results indicate that the main effect of H-ZSM-5 has been observed on the amount of water and oxygen for all bio-oil samples at three different temperatures, where a significant reduction has been achieved compared to non-catalytic bio-oil samples. In addition, a significant viscosity reduction has been reported compared to non-catalytic bio-oil samples, and less viscous bio-oil samples have been produced by catalytic pyrolysis. Furthermore, the obtained results show that the heating values have been increased for upgraded bio-oil samples compared to non-catalytic bio-oil samples. The GCMS analysis of the catalytic bio-oil samples (H-ZSM-5) indicates that toluene and methanol have shown very similar behavior in extracting bio-oil samples in contrast to non-catalytic experiments. However, methanol performed better for extracting chemicals at a higher temperature.

Keywords: biomass; bio-oil; upgrading; catalytic pyrolysis; lignin; fractionation



Citation: Abdulkhani, A.; Zadeh, Z.E.; Bawa, S.G.; Sun, F.; Madadi, M.; Zhang, X.; Saha, B. Comparative Production of Bio-Oil from In Situ Catalytic Upgrading of Fast Pyrolysis of Lignocellulosic Biomass. *Energies* **2023**, *16*, 2715. <https://doi.org/10.3390/en16062715>

Academic Editor: Antigoni Margellou

Received: 12 December 2022

Revised: 26 February 2023

Accepted: 28 February 2023

Published: 14 March 2023



Copyright: © 2023 by the authors. Licensee MDPI, Basel, Switzerland. This article is an open access article distributed under the terms and conditions of the Creative Commons Attribution (CC BY) license (<https://creativecommons.org/licenses/by/4.0/>).

1. Introduction

In the last few decades, environmental issues from the unreasonable consumption of fossil-based fuels have led to ever-growing concerns regarding greenhouse gas emissions. Different strategies have been proposed to gradually substitute conventional fossils, including bio-based fuels from bioresources, such as biomass. Biomass has been recognized as one of the potential sources of renewable materials for the production of energy and fuels. Lignocellulosic biomass, composed of cellulose, hemicellulose, and lignin, can be converted to different biofuels through biochemical and thermochemical pathways [1]. Pyrolysis is one of the thermochemical routes established to produce bio-oil from biomass sources. Generally, pyrolysis is a thermal decomposition process of biomass in the absence

of oxygen to a range of liquid, solid, and gaseous products, namely bio-oil, biochar, and fuel gas [2]. The condensed volatiles of this process is considered as bio-oil gas [3]. The solid pyrolysis product is known as biochar and is rich in carbon content between 65 and 90% [4]. In other words, heavy hydrocarbon molecules of biomass are converted to low-weight hydrocarbons in the pyrolysis process, and almost any type of bio-based materials can be used as feedstock for the production of bio-oil through the pyrolysis process. In addition to feedstock variability, pyrolysis can be performed at atmospheric pressure. Bio-oil is a dark brown liquid with a pungent odor that contains aromatic hydrocarbons, phenol derivatives, alkanes, and minute amounts of ketone, amine, alcohol, ester, and ether [5]. Numerous studies on bio-oil production have been conducted to investigate the effects of feedstock and operating parameters on the distributions of the pyrolysis bio-oil compositions. Ligno-cellulosic biomass is a promising feedstock source for producing high-quality pyrolysis products, including phenolics, ketones, aromatics, and furans. Table 1 reviews the different types of raw materials for bio-oil production.

Table 1. Review of the pyrolysis conditions of some bio-based materials.

No.	Feedstock	Temperature (°C)	Bio-Oil Yield	Catalyst	Composition	Reference
1	Algal biomass	-	-	-	pyrazines, furans, and pyridines	[6]
2	Sisal residue	450	-	-	fats, waxes, alkaloids, proteins, phenolics, simple sugars, pectins, gums, and resins	[7]
3	Peanut shells	600	-	-	ketones and anhydro sugars, aromatics	[8]
4	Bamboo residues	-	93.83 mg/g	H-ZSM-5	Aromatics (2-Methoxy-4-vinylphenol)	[9]
5	Olive pomace	340	36.9 wt%	-	Phenolics	[10]
6	Olive stones	600	-	-	Guaiacol and 2-methoxy-4-methyl substituted phenol	[11]
7	Lignocellulosic biomass	-	-	H-ZSM-5	monocyclic aromatics	[12]
8	Biomass	-	47–52 wt%	CeO ₂	Furfural, furfural alcohol, furan	[13]
9	Agricultural residues	-	-	-	benzene, toluene, xylene, ethene, propene	[14]
10	Eucalyptus residues	480	30 wt%	-	Hydrocarbons	[15]
11	Macadamia Nutshell	471.21	43.37 wt%	-	phenol, aromatics, and alcohol	[16]
12	Poplar sawdust, cellulose, and lignin	250–550	-	-	anhydrate sugars, ketones, aldehydes, and phenolics	[17]
13	Food waste	400	34.90 wt%	-	N-compounds, hydrocarbons, and carboxylic acid	[18]
14	Pitch pine biomass	500	65.5 wt%	-	levoglucosan, furfural, and guaiacol	[19]
15	Banana pseudo-stem	500	39.4 wt%	-	phenols	[20]

Table 1. Cont.

No.	Feedstock	Temperature (°C)	Bio-Oil Yield	Catalyst	Composition	Reference
16	Walnut shells (WS)	550	44.7 wt%	-	feedstock for furnaces	[21]
17	lignocellulosic biomass	700	-	-	aromatics	[22]
18	Aesculus chinensis Bunge Seed	-	-	Fe ₂ O ₃ and NiO	1-hydroxy-2-propanone, acetic acid, and furfural	[23]
19	sunflower seed hulls (SSH)	450	33 wt%		furfural enriched bio-liquid	[24]
20	Chicken litter	500	-	dolomite and ZSM-5	phenolic compounds	[25]

Fast pyrolysis is a well-known procedure for bio-oil production from biomass where the quick quenching at the end of the process leads to the production of liquid bio-oil, bio-char, and non-condensable gaseous products of 60–70%, 12–15%, and 13–25%, respectively [26]. Slow pyrolysis requires a lower heat transfer rate, resulting in lower bio-oil yields of 30–45 wt% than fast pyrolysis and a high char level of 34–63 wt% [27]. The composition of pyrolysis products is defined by the source, quality of the biomass, and operating parameters [28]. Bio-oil from biomass pyrolysis has undesirable properties due to the complexity of biomass composition. The presence of water, acids, and aldehydes causes poor bio-oil quality compared to petroleum-based fuels due to high acidity, water content, low heating value (LHV), high corrosiveness, and instability [29]. The presence of water in bio-oil adversely affects bio-oil storage, leading to phase separation and reducing heating values (HHV and LHV). Moreover, the production of organic acids during the thermal degradation of biomass decreases the pH value, which leads to the corrosion of facilities in possible applications. Therefore, the bio-oil quality must be enhanced by eliminating water, acid, and hazardous components [30].

Different physical and chemical upgrading methods have been reviewed and discussed in the previous publication for bio-oil upgrading [31]. Catalytic upgrading methods include hydrodeoxygenation (HDO), zeolite cracking, and steam reforming. The HDO reduces the oxygen content by converting it to deoxygenated products under a high-pressure hydrogen stream. Dehydration, hydrogenation, decarboxylation, hydrogenolysis, and hydrocracking are typical potential reactions during the HDO upgrading method. One of the drawbacks of the HDO upgrading method is the high cost of operation, including hydrogen stream, high pressure, and catalyst deactivation, which prevents the implementation of these methods on a commercial scale [32]. Steam reforming is the method of upgrading where the hydrocarbons are converted into syngas with steam reaction at a high temperature.

Catalytic upgrading has been favored due to the benefits of operating at atmospheric pressure and without any hydrogen stream [33]. Cracking, hydrocracking, decarboxylation, decarbonylation, deoxygenation, hydrodeoxygenation, and hydrogenation are the proposed general reactions in fast catalytic pyrolysis (CFP) [34]. A different article has reviewed the reaction pathway of catalytic pyrolysis of woody biomass and the effect of a catalyst on product distribution [31].

Catalytic pyrolysis can be performed via two different reactor configurations. The catalyst can be physically mixed with biomass (in situ) and added to the reactor, or the catalyst can be loaded into the outlet of the pyrolyser to upgrade the volatile product gas before the condensation process has taken place (ex situ configuration).

Different types of catalysts have been reviewed in the literature for catalytic pyrolysis of biomass. However, solid catalysts are interesting due to their ability to modify the products through decarboxylation, decarbonylation, dehydration, cracking, and isomerization. Zeolites, solid acid catalysts, have gained significant attention due to their acidity

and ability to produce aromatic compounds during catalytic pyrolysis [35]. The ability of zeolites to trap the molecules via their open, crate structure makes them common catalysts in modification reactions. Hydrothermal stability, less corrosion, ease of use, and set up in continuous processes of H-ZSM-5, make it an excellent endothermic catalyst compared to other zeolite catalysts, such as HMOR, HBEA, and USY. Moreover, H-ZSM-5 exhibits a higher heat transfer and high conversion rate compared to other zeolites [35].

There has been an increasing demand for applications of upgraded bio-oil for extraction and valorization of the extracted aromatic chemicals and a range of alkanes from bio-oil as a renewable source of energy. It has been approved that pyrolysis liquid is a source of broad organic chemicals, and over 300 different types of compounds have been identified in wood-fast pyrolysis bio-oil [36]. The chemical groups, e.g., alcohols, aldehydes, esters, ketones, phenolics, sugars, acids, and aromatics, have been identified in this study by the solvent extraction approach. Figure 1 illustrates the possible applications of upgraded bio-oil fast pyrolysis. Upgraded bio-oil can be used as a source of oil (fuel) or as a power source, such as diesel in numerous applications, boilers, and turbines for electricity generation and biochemical production. Moreover, it can be used to produce carbon-based high value-added products, including graphene and carbon fibers. In addition, the obtained components in bio-oil belong to jet fuel hydrocarbon groups, in which alkanes and aromatics are the main jet-fuel-ranged hydrocarbons [37]. Furthermore, the extracted chemicals can be used to produce resins, fertilizers, adhesives, phenol-formaldehyde-type resins, etc. [3]. However, the amounts and compositions of the bio-oil components are strongly dependent on the biomass type, production approach, and operating conditions [2].

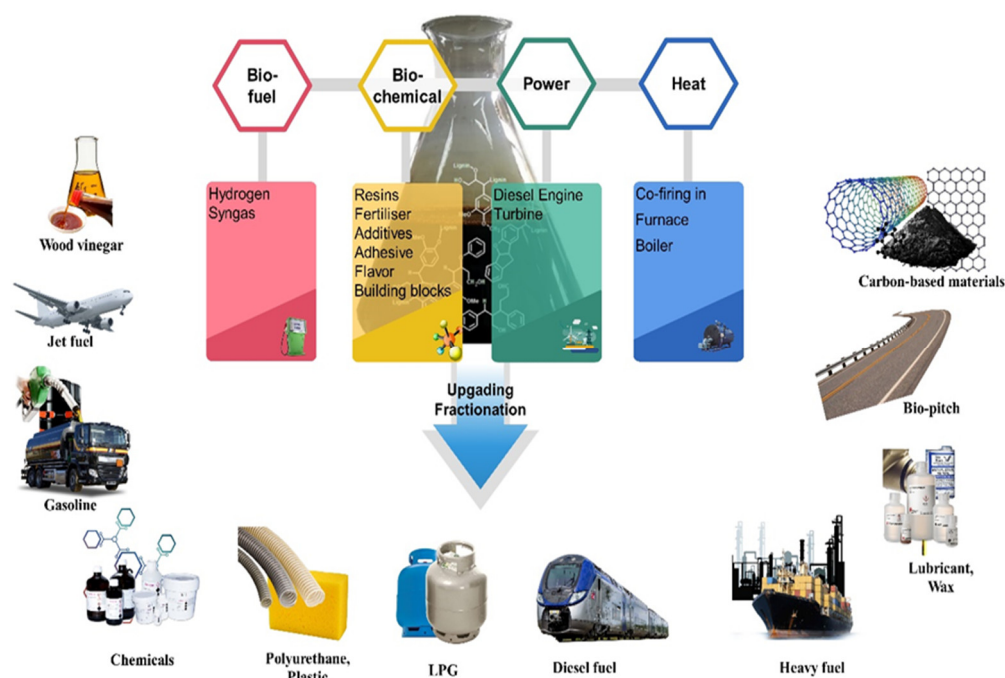


Figure 1. Products and different applications of bio-oil.

This research aims to perform extensive bio-oil characterization obtained from catalytic fast pyrolysis (CFP) of lignocellulosic biomass at three different temperatures using the H-ZSM-5 catalyst. To achieve the main target of this research, two different types of lignocellulosic biomass (Kraft lignin and wood chips) have been selected for catalytic bio-oil production and characterization. Different characterization techniques have been investigated in this study. The fractionation method was used to identify the chemical composition of bio-oil samples after catalytic pyrolysis experiments by gas chromatography with mass spectroscopy (GCMS). Other characterization techniques, e.g., water content,

viscosity, pH, elemental analysis, and bomb calorimetry, have been conducted, and the obtained results have been compared to non-catalytic pyrolysis.

The present study performed a catalytic fast pyrolysis process for upgrading bio-oil at three production temperatures for two different biomasses. Next, a multi-step solvent extraction method has been used for refining the yields by removing the impurities and determining the composition of chemicals obtained by catalytic fast-pyrolysis bio-oil.

The outcome of the published literature generally focuses on bio-oil production. However, many properties of fast pyrolysis of biomass processes, such as characterizing bio-oil parameters and upgrading, require further study and investigation. The novelty of this study is to achieve intensive bio-oil characterization from a catalytic fast pyrolysis process for the separation of bio-chemicals from two different feedstock sources.

2. Materials and Methods

2.1. Materials

The commercial Kraft lignin supplied by Sigma Aldrich (Munich, Germany) (softwood lignin), and the wood chips sample from Spruce (softwood) were employed for this study. The feedstocks (Kraft lignin and wood chips) were dried in an oven for 12 h at 373 K to remove moisture before pyrolysis experiments. A commercial-grade zeolite, ZSM-5, ammonium, Alfa Aesar™ (Haverhill, MA, USA), with a mole ratio ($\text{SiO}_2/\text{Al}_2\text{O}_3$) of 23:1 and surface area of $425 \text{ m}^2/\text{g}$ was procured from Fisher Scientific, Loughborough, UK.

2.2. Catalyst Preparation

ZSM-5 was obtained in ammonium form and was changed to proton form via the calcination method. In this process, 100 g of ZSM-5 was added to ammonium hydroxide (NH_4OH), stirred for 20 min, and filtrated. The mixture was calcined at 873 K for 6 h in airflow for conversion to its protonated form, H-ZSM-5 [38–41].

2.3. Methods

2.3.1. Catalyst Characterization

The morphologies and crystal sizes of zeolite catalyst were investigated before and after calcination treatment by X-ray diffraction (XRD) and field emission scanning electron microscope (FE-SEM) images analyses. The analyses were performed on FESEM Model Mira3 TeScan-XMU using platinum coating, and XRD analyses were performed with copper anode (Cu) and 40 kV voltage.

2.3.2. In Situ Catalytic Pyrolysis Experiment

A fixed bed, bench-scale pyrolysis reactor was designed and fabricated for catalytic and non-catalytic bio-oil production (Figure 2), whereas the feedstock (Kraft lignin and wood chips) was added separately to the pyrolyser for each experiment. The required heat for the pyrolysis process was provided by an external electrical power. Nitrogen gas was used as a carrier gas to provide inert conditions for this process. In this study, the H-ZSM-5 catalyst was physically mixed with feedstock (1:4; $w:w$), and then the mixture of biomass and catalyst was introduced to the reactor (pyrolyser). The experiments were carried out at 673, 773, and 873 K. Figure 2 illustrates the feedstock preparation for in situ catalytic pyrolysis. The non-catalytic and catalytic experiments were performed under the same conditions. The detailed method for the fabrication of the pyrolyser reactor and the production process of bio-oil for the non-catalytic test is described in a different article [3]. To study the effect of the upgrading method (catalytic pyrolysis), the obtained results were compared with non-catalytic (thermal) pyrolysis. The schematic of the experimental upgrading setup is shown in Figure 2. The obtained catalytic bio-oil samples were coded and characterized to identify the properties of the upgraded bio-oil samples.

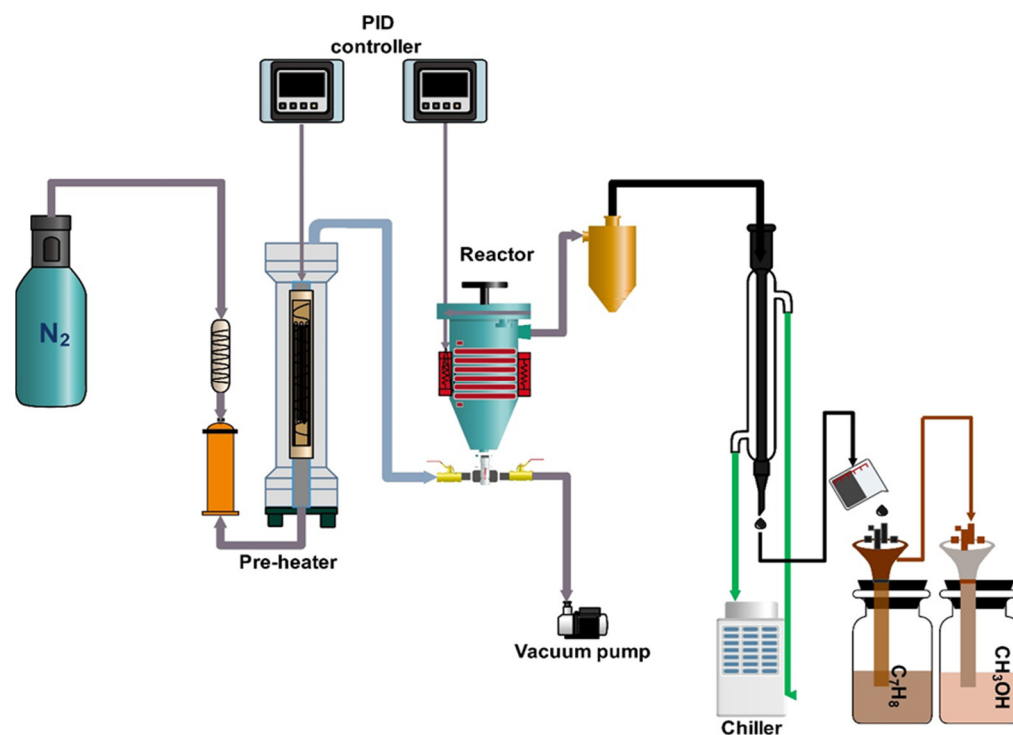


Figure 2. Schematic of the experimental setup for catalytic pyrolysis process (Adapted from [42]).

2.4. Upgraded Bio-Oil Characterization

2.4.1. Fractionations of Bio-Oil

The fractionation method was employed to determine the chemical composition of bio-oil samples after the catalytic pyrolysis experiments. Bio-oil (4 mL) was extracted with toluene (115 mL) to obtain toluene-soluble and toluene-insoluble fractions. Then, the toluene-insoluble fraction was mixed with methanol (115 mL) to obtain MeOH-soluble and MeOH-insoluble fractions. The toluene- and methanol-soluble fractions were concentrated with a rotary evaporator to be injected into the GCMS.

2.4.2. GCMS Analysis of Upgraded Bio-Oil Fractionations

The bio-oils were analyzed with a GCMS-QP2010S Shimadzu gas chromatography with mass spectroscopy (GCMS). A mild-polarity phase, 14% cyanopropylphenyl polysiloxane; column (30 m × 0.25 mm ID) was used. The GC oven temperature was held at 323 K for 2 min and then programmed to 563 K at 5 K min⁻¹. The injection dose was 1 μL, and the injector temperature was 568 K with split mode. Helium was used as a carrier gas with a 0.90 mL/min flow rate.

2.4.3. Water Content, Viscosity, pH, and Heating Values

The water content analysis of the bio-oil samples was obtained by a Karl Fischer V20 volumetric titrator (Mettler Toledo, Ohio, United States) according to ASTM E203 (2001) using dry methanol as the solvent. The average of three runs for each sample was reported. The upgraded bio-oil samples' pH values were measured using PHM240 at 298 K. The bio-oil samples' viscosity values were measured using Bohlin Gemini 2 at 313 K. The heating values were obtained using an oxygen bomb calorimeter (Parr 6100), according to ASTM D240 (2009).

2.4.4. Elemental Analysis (CHNO)

C, H, S, and O contents of bio-oil samples were determined using a CE-440 elemental analyzer.

2.4.5. Thermogravimetric Analysis

Thermogravimetric analysis was performed using a 209 F3 Tarsus TGA analyzer. A heating rate of 10 °C/min under a nitrogen gas atmosphere with a flow rate of 40 mL/min were used to determine the thermogravimetric degradation of samples.

3. Results and Discussion

3.1. Catalyst Characterization

The morphology of zeolite catalysts before (ZSM-5) and after treatment (H-ZSM-5) was investigated using field emission scanning electron microscope (FE-SEM) images and X-ray diffraction (XRD) analysis. The SEM images of ZSM-5 and H-ZSM-5 are shown in Figure 3. The results show that H-ZSM-5 has irregular and spherical morphology, which is very similar to its ammonium type (ZSM-5), indicating that no change in physical morphology occurred during the heat treatment. The XRD analysis results have shown that the spectra of the two samples are very similar (identical). In other words, the molecular structure and the catalyst crystallinity were not destroyed during the calcination treatment. The XRD pattern of ZSM-5 and H-ZSM-5 shows very similar diffraction patterns. These results agree with those obtained by Zheng et al. [43] and Tursunov et al. [41].

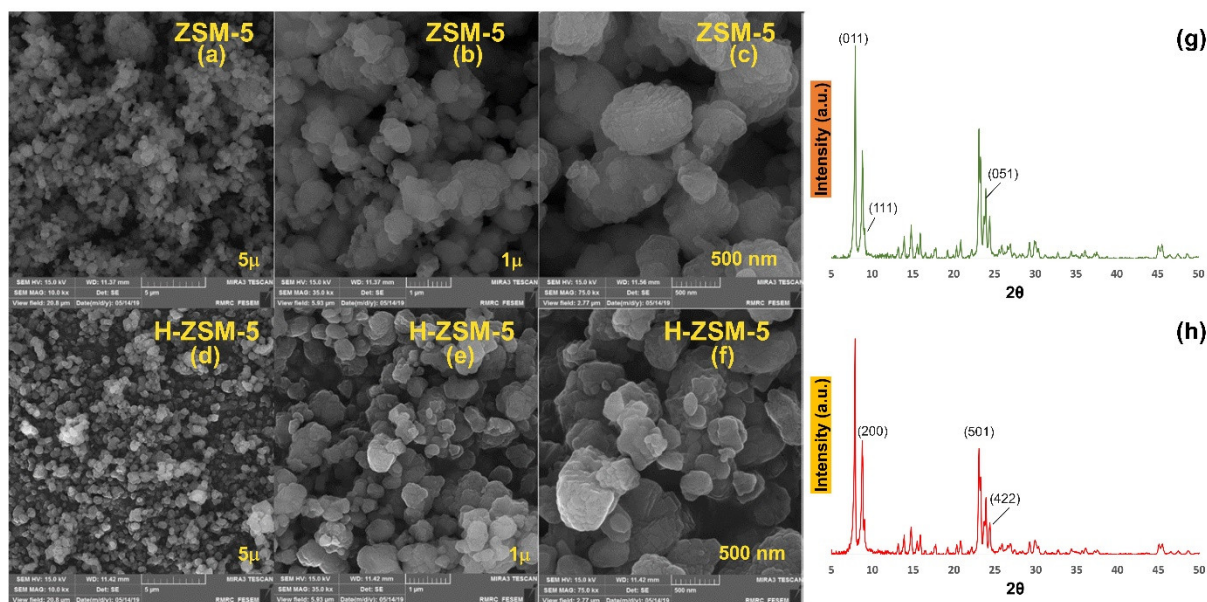


Figure 3. SEM images of ZSM-5, before calcination: (a–c); H-ZSM-5, after calcination: (d–f); and XRD pattern of ZSM-5 and H-ZSM-5: (g,h).

3.2. Product Yields

The bio-oil yields of the catalytic fast pyrolysis (C) of two different types of feedstocks at three different temperatures are shown in Table 2. The same table shows the non-catalytic pyrolysis (NC) results of the bio-oil samples from the same feedstocks under the same experimental conditions. The effect of H-ZSM-5 on bio-oil upgrading is presented in Table 2 and compared with non-catalytic experiments, and the product yields, liquid, char, and gas were determined experimentally and are presented. Different pyrolysis temperatures affecting the yield of the products include bio-oil, biochar, and syngas. The range of values of bio-oil yields shows no significant difference between catalytic and non-catalytic fractions. However, the general trend shows a decrease in catalytic bio-oil yields. It was notable that the formation of char affects the bio-oil yield. For instance, the highest values of the biochar were reported for lignin for both non-catalytic and catalytic bio-oils. The biochar yield for non-catalytic bio-oil from Sigma Kraft Lignin at 773 K was 58.0 wt%, which can be considered as the main reason for the lower bio-oil yields from lignin in

comparison to bio-oil from wood chip samples. Similar observations were stated in the literature by Apunda and Ogenga 2016 [38].

Table 2. Product yields of four different samples of catalytic (C) and non-catalytic (NC) bio-oil.

Sample ID	Product Yields (%)					
	Bio-Oil		Biochar		Syngas	
	NC	C	NC	C	NC	C
Lignin-673 K	24.3	30.1	56.2	51.7	19.4	18.1
Lignin-773 K	30.2	31.4	58.0	53.5	11.7	15.0
Lignin-873 K	26.0	25.5	52.2	50.8	21.7	23.6
S-wood-673 K	57.4	50.9	23.2	24.3	19.3	24.7
S-wood-773 K	65.4	61.3	18.5	18.2	16.0	20.4
S-wood-873 K	71.1	69.9	11.4	13.0	17.3	17.0

The lowest amount of biochar yield was experienced for the bio-oil from wood samples. The trend of syngas yields was unpredictable for catalytic and non-catalytic bio-oil samples, but the general trend exhibits an overall increase in syngas yields with an increase in temperature. The highest bio-oil yield was found to be from softwood at 873 K for both catalytic and non-catalytic experiments.

3.3. Physical Properties of Upgraded Bio-Oil

3.3.1. Elemental Analysis

Table 3 illustrates the elemental analysis and the presence of O:C, C:H ratios of the obtained catalytic and non-catalytic bio-oils, since the hydrogen content of the bio-oils was close to each other (5.4–7.4%), and C:H ratio was used to evaluate the bio-oil carbon content. Generally, samples with a low O:C ratio have low oxygen and high carbon, retaining the highest heating value. The raw bio-oil has a low amount of carbon for lignin (47.7–68.8%) and wood chips (32.5–55.8%) bio-oil samples and a high amount of oxygen for lignin (22.9–44.3%) and softwood (37.2–62.8%) bio-oil samples, indicating that this procedure led to the loss of carbon in the form of uncondensed gases as carbon monoxide (CO). This conclusion is reinforced by GCMS data that showed the withdrawal of some chemical compounds. H-ZSM-5 effectively decreased the oxygen content of both lignin and softwood pyrolysis oil. The oxygen content of H-ZSM-5-catalyzed bio-oil from lignin and wood chips decreased despite having a high amount of dissolved water. The H-ZSM-5-catalyzed lignin bio-oil at 773 K had the highest C:H ratio and the least O:C ratio, indicating that this sample possessed the highest heating value. The overall conclusion from these results shows that H-ZSM-5 was efficient in transforming the pyrolysis vapors to partially deoxygenated liquid fuel.

Table 3. Elemental analysis of non-catalytic (NC) and catalytic (C) bio-oil samples.

Sample ID	C		H		S		O		C/H		O/C	
	NC	C	NC	C	NC	NC	NC	C	NC	C	NC	C
Lignin-673 K	47.7	35.6	6.9	5.4	1.1	44.3	29.5	6.9	6.6	0.9	0.8	
Lignin-773 K	68.5	63.8	6.6	6.9	2.0	22.9	14.6	10.3	9.2	0.3	0.2	
Lignin-873 K	60.8	64.4	7.1	7.0	1.5	30.5	28.6	8.5	9.2	0.5	0.4	
S-wood-673 K	32.5	50.0	6.6	7.4	0.6	60.4	42.6	5.0	6.8	1.9	0.9	
S-wood-773 K	30.3	47.2	6.5	7.1	0.4	62.8	45.7	4.7	6.6	2.1	1.0	
S-wood-873 K	55.8	46.3	6.3	7.3	0.7	37.2	36.4	8.9	6.3	0.7	0.8	

3.3.2. Water Content, Viscosity, pH, and Heating Values

A comparison of catalytic and non-catalytic values of water content, pH, and viscosity of obtained bio-oils is presented in Table 4. For all bio-oil samples, the water content was observed to be increased upon catalytic treatment regarding the non-catalytic bio-oil

samples. The catalyzed bio-oils had varied amounts of dissolved water ranging from 11.2–14.2% for lignin and 41.8–56.7% in softwood samples at different temperatures. The raw bio-oil had the water content, i.e., 5.3–7.2% and 26.5–32.5% in lignin and softwood samples, respectively, indicating that pyrolysis encourages secondary condensation reactions that lead to increased water content after the catalytic reactions. Increases in the polarity of bio-oil could also be due to the presence of dissolved water.

Table 4. Water content, pH, and viscosity of the non-catalytic (NC) and catalytic (C) bio-oil samples.

Sample ID	Water Content (%)		pH		Viscosity (cP)	
	NC	C	NC	C	NC	C
Lignin-673 K	5.3	11.2	5.0	5.6	20.4	33.6
Lignin-773 K	4.8	10.4	5.3	5.7	28.4	36.2
Lignin-873 K	7.2	14.2	5.6	6.2	74.9	58.9
S-wood-673 K	32.5	56.7	2.3	2.6	80.5	37.1
S-wood-773 K	26.5	48.6	2.4	2.7	86.6	28.3
S-wood-873 K	31.2	41.8	2.5	3.0	95.4	21.9

The high content of water and organic acid in bio-oil is the reason for low pH values (pH 2.3–2.5). On the other hand, the pH values for the non-catalytic bio-oil of lignin were found between 5.03 and 5.6. It was found that the pH values of the upgraded oils increased compared with non-catalytic bio-oils.

A great viscosity reduction was observed for upgraded bio-oil from softwood at a pyrolysis temperature of 773 and 873 K. Figure 4 illustrates the non-catalytic and catalytic bio-oil samples' heating values indicating that the heating values of upgraded bio-oil samples increased compared to non-catalytic results. However, bio-oil from lignin samples shows a higher increase in HHV in catalytic pyrolysis compared to bio-oil samples from wood chips. The viscosities of the catalyzed bio-oils were found to be a proper function of catalyst activity. The bio-oil with the least viscosity was obtained from pyrolysis of lignin samples regarding the obtained bio-oil from softwood, resulting from the presence of polysaccharide chains from partial degradation of cellulose.

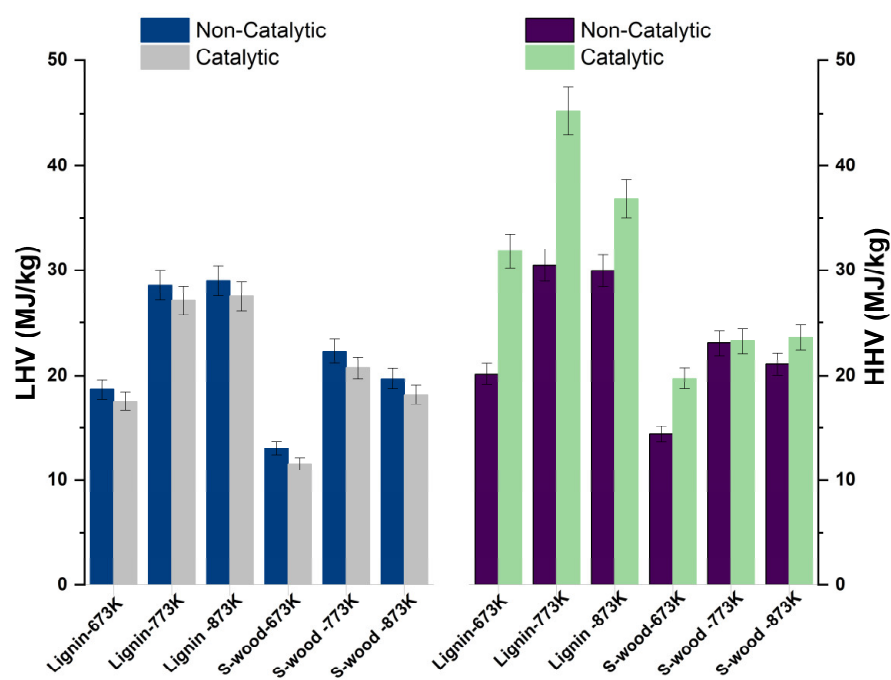


Figure 4. Lower heating value (LHV) and higher heating value (HHV) of non-catalytic and catalytic bio-oil samples.

3.4. GCMS Analysis of Different Fractions of Upgraded Bio-Oil Samples

The fractionation method was employed to determine the chemical composition of bio-oil samples. The extracted fractions of the upgraded bio-oil samples were determined by GCMS analysis. The chemical composition of the bio-oils was evaluated by grouping the compounds into lignin-derived and polysaccharide-derived components and discarding the moieties obtained from the extractives. The chemical compositions and peak identification of extracted toluene, which is an upgraded bio-oil from Kraft lignin at three different temperatures of 673, 773, and 873 K, are presented in Table 5. The corresponding chromatograms for each fraction are provided in Supplementary Materials (Figure S1). Comparing the non-catalytic fractions with catalytic fractions results indicate that toluene has a similar performance in the separation of bio-oil compounds [3]. Toluene can be considered as an efficient solvent for separating a range of non-polar compounds. As shown in Table 5, different phenolic and aromatic compounds were the most dominant compounds separated by toluene fraction.

Table 5. GCMS chromatogram resulting from H-ZSM-5 upgraded bio-oil from lignin toluene-soluble corresponding components.

No.	Retention Time	Relative Intensity			Compound	Chemical Structure
		673 K	773 K	873 K		
1	14.3	17.5	8.6	5.1	Guaiacol	
2	16.4	1.4	11.4	6.4	<i>p</i> -Creosol	
3	17.6	20.3	4.8	1.7	<i>o</i> -Xylenol	
4	19.5	14.7	7.7	2.2	<i>p</i> -Ethylguaiacol	
5	21.7	4.1	1.8	-	Cerulignol	
6	22.3	1.8	2.8	-	3,4-Dimethoxyphenol	
7	24.2	4.9	3.4	1.9	Eugenol	
8	26.6	2.1	1.6	-	Vanillin	
9	27.7	2.9	2.2	-	Guaiacylacetone	
10	30.5	2.6	2.0	1.0	Mandelic acid	
11	43.2	2.2	1.5	-	Vanillyl alcohol	

The thermal degradation of phenyl propane units in lignin led to low molecular weight monolignol-based compounds. Analysis of the toluene-extracted fraction shows that the obtained bio-oil from lignin at 673, 773, and 873 K led to the disincorporation of lignin to guaiacol, greosol, gylenol, gthylguaiacol, cerulignol, 3,4-dimethoxyphenol, eugenol, vanillin, guaiacylacetone, mandelic acid, and vanillyl alcohol with different concentrations. The relative abundance of most obtained components was surprisingly decreased by increasing the pyrolysis temperature from 673 to 873 K. For example, the relative abundance

of guaiacol was decreased from 17.5 to 5.1% by increasing the temperature from 673 to 873 K, respectively.

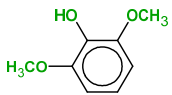
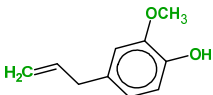
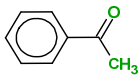
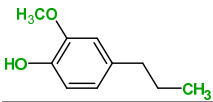
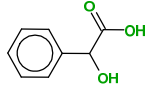
The same trend was observed for xylene, ethylguaiacol, cerulignol, eugenol, vanillin, guaiacylacetone, mandelic acid, and vanillyl alcohol. Regarding the increase in carbon content (Table 3—elemental analysis), it seems that high molecular weight compounds were discarded due to the low solubility of produced condensed structures from hydrodeoxygenation of lignin moieties in toluene.

According to Table 6, which represents the MeOH-soluble fractions from catalytic pyrolysis of Kraft lignin, almost the same performance and separation pattern is observed for MeOH-soluble fractions compared to non-catalytic results [3]. The corresponding chromatograms for each fraction are provided in Supplementary Materials (Figure S1). Aromatic acids and phenolics were the main detected compounds by GCMS. Compared to the toluene extracted fraction, methanol extraction contained more phenolic moieties. Fumaric acid, rosolic acid, mequinol, cresol, 4-ethylcatechol, xylene, ethylguaiacol, ethyl-*m*-cresol, syringol, eugenol, acetophenone, propylguaiacol, and mandelic acid were the main identified components. The results confirmed that MeOH extracted more chemicals at higher temperatures of 773 and 873 K.

Table 6. GCMS chromatogram resulting from H-ZSM-5 upgraded bio-oil from Kraft lignin MeOH-soluble corresponding components.

No.	Retention Time	Relative Intensity			Compound	Chemical Structure
		673 K	773 K	873 K		
1	3.6	21.5	-	-	Fumaric acid	
2	14.0	2.4	5.1	6.9	Rosolic acid	
3	14.3	-	7.6	6.2	Mequinol	
4	16.3	-	-	4.4	<i>m</i> -Cresol	
5	17.2	9.1	10.5	8.7	4-Ethylcatechol	
6	17.6	-	5.1	6.2	<i>o</i> -Xylenol	
7	19.5	5.2	6.5	4.7	<i>p</i> -Ethylguaiacol	
8	19.9	-	2.0	1.9	Ethyl- <i>m</i> -cresol	

Table 6. Cont.

No.	Retention Time	Relative Intensity			Compound	Chemical Structure
		673 K	773 K	873 K		
9	22.4	-	6.9	3.7	Syringol	
10	24.3	1.9	3.1	4.9	Eugenol	
11	26.7	-	1.8	1.1	Acetophenone	
12	27.7	-	1.5	1.4	<i>p</i> -Propylguaiacol	
13	30.5	-	2.9	1.8	Mandelic acid	

Phenols are high-interest products from biomass pyrolysis due to their wide range of applications as value-added chemicals. Phenols may form through the thermal cleavage/catalytic cracking of the O-C and C-C bonds in 4-hydroxyphenyl and guaiacols moieties of the lignin polymer or a stepwise reaction including the dehydration-hydrolysis of vanillins and guaiacols to diols and then to phenols [44]. Therefore, the relatively high amount of phenols in the upgraded bio-oils indicates the ability of H-ZSM-5 to crack the heavier compounds. Cracking down the phenolics to hydrocarbons or carbon residue but not entirely to non-condensed gases has also been reported elsewhere [44].

The toluene- and MeOH-soluble compounds from GCMS analysis of wood chip's fast pyrolysis at three different temperatures of 673, 773, and 873 K are presented in Tables 7 and 8. The corresponding chromatograms for each fraction are provided in Supplementary Materials (Figure S2). According to Tables 7 and 8, the obtained components originated mainly from lignin and polysaccharides fractions of softwood chips. Methanol achieved a suitable extraction for this type of bio-oil. A wide range of compounds, including C3–C10, were extracted in these fractions. It was found that methanol has the same performance in extracting different chemical families in softwood fractions at different temperatures.

Table 7. GCMS chromatogram resulting from H-ZSM-5 upgraded bio-oil from Spruce (softwood) toluene-soluble corresponding components.

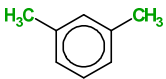
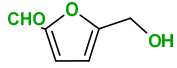
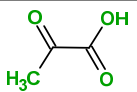
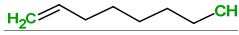
No.	Retention Time	Relative Intensity			Compound	Chemical Structure
		673 K	773 K	873 K		
1	5.9	4.3	-	-	<i>m</i> -Xylol	
2	6.9	4.8	1.7	5.2	Hydroxymethylfurfural	
3	8.3	1.9	-	1.9	Pyruvic acid	
4	13.2	1.8	2.5		Octene	

Table 7. Cont.

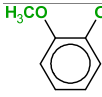
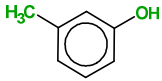
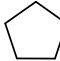
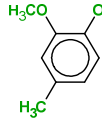
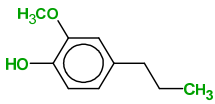
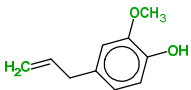
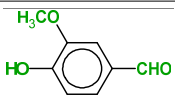
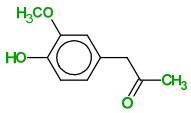
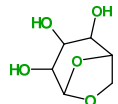
No.	Retention Time	Relative Intensity			Compound	Chemical Structure
		673 K	773 K	873 K		
5	14.2	5.4	8.4	6.8	<i>p</i> -Guaiacol	
6	16.4	4.2	1.4	5.6	<i>m</i> -Cresol	
7	17.0	-	3.0	1.5	Cyclopentane	
8	17.1	11.3	13.5	-	<i>p</i> -Cresol	
9	19.4	4.8	7.7	-	<i>p</i> -Ethylguaiacol	
10	24.2	3.0	4.8	1.3	Eugenol	
11	26.6	-	1.6	-	Vanillin	
12	27.7	-	2.3	-	Guaiacylacetone	
13	30.1	-	2.3	-	Levogluconan	

Table 8. GCMS chromatogram resulting from H-ZSM-5 upgraded bio-oil from Spruce wood chips MeOH-soluble corresponding components.

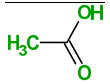
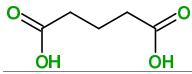
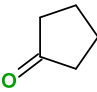

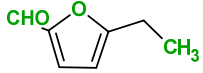
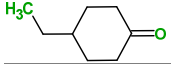
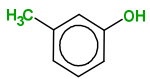
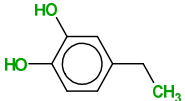
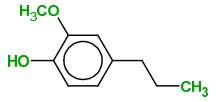
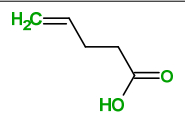
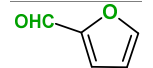
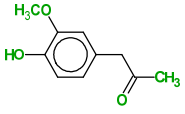
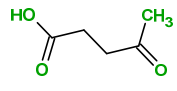
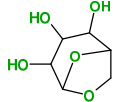
No.	Retention Time	Relative Intensity			Compound	Chemical Structure
		673 K	773 K	873 K		
1	3.4	-	-	2.7	Acetic acid	
2	6.6	-	1.3	-	Glutaric acid	
3	13.3	4.1	3.5	2.0	Cyclopentanone	
4	14.0	2.0	2.1	4.3	Phenol	

Table 8. Cont.

No.	Retention Time	Relative Intensity			Compound	Chemical Structure
		673 K	773 K	873 K		
5	14.3	4.6	3.7	2.1	5-Ethylfurfural	
6	15.7	1.2	-	-	4-Ethylcyclohexanone	
7	16.4	1.4	-	2.4	<i>m</i> -Cresol	
8	17.2	12.9	12.0	4.9	4-Ethylcatechol	
9	19.4	3.5	2.5	2.2	<i>p</i> -Ethylguaiacol	
10	20.3	1.5	1.7	-	Pentenoic acid	
11	22.0	1.3	1.4	-	Furfural	
12	27.7	1.7	1.8	-	Guaiacylacetone	
13	29.6	1.5	2.3	-	Levulinic acid	
14	30.4	2.1	6.2	2.6	Levogluconan	

Generally, fast pyrolysis of softwood chips led to gases, organics, and solid char formation by homogenous thermal decomposition. The dehydration of volatile organics at elevated temperatures led to water and dehydrated products. Zeolite catalysts are commonly known for their shape-selective catalytic reactions [45]. Upon contact with active sites of the H-ZSM-5, the dehydrated products undergo different reactions, including isomerization oligomerization, decarboxylation, dehydrogenation, and decarbonylation [46–48], leading to the formation of non-condensed gases (CO, CO₂, H₂), low molecular weight oxygenates aliphatic, water, aromatic hydrocarbons, and coke [49]. The catalytic effect of H-ZSM-5 in transforming the volatile organics into hydrocarbons mainly occurs through carbocation/carbenium ion reaction intermediates [47]. The Brønsted acid sites of the H-ZSM-5 donate an acidic proton to the pyrolytic substrate, such as an oxygenated compound or a hydrocarbon, forming a carbocation intermediate. The proposed reaction pathways of lignocellulose catalytic pyrolysis with H-ZSM-5 are illustrated in Figure 5.

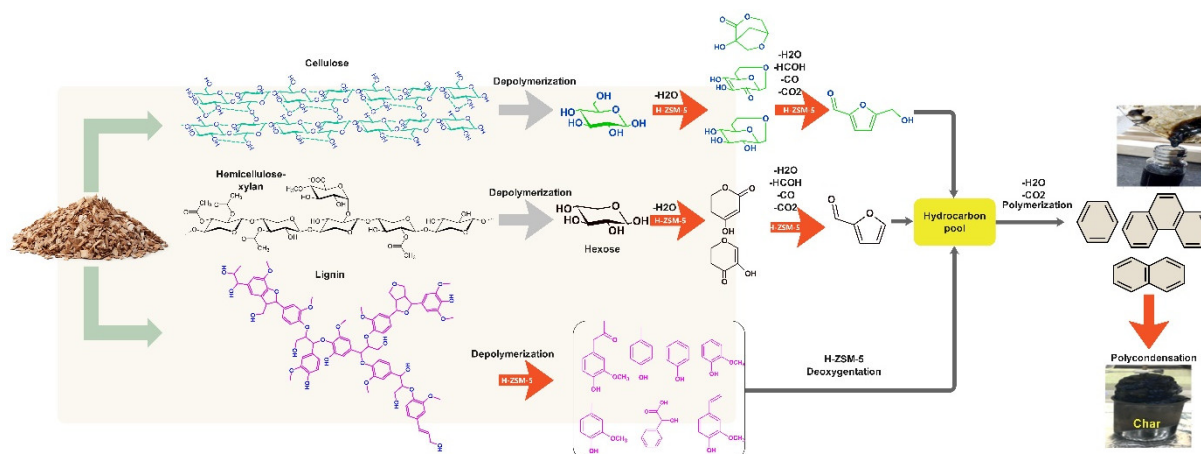


Figure 5. Proposed reaction pathways of lignocellulose catalytic pyrolysis with H-ZSM-5.

In this context, the polysaccharides of wood chips undergo the depolymerization and dehydration reaction leading to the formation of anhydrosugars, lower molecular weight furans, and hydrocarbons. The high Brønsted acidity of H-ZSM-5 promotes the extensive dehydration of disincorporated monosaccharides to form furfural and 5-methyl furfural (HMF) [28,31,32,47,50]. Moreover, pyrolysis of softwood chips results in the depolymerization of lignin polymer into mainly guaiacyl (4-hydroxy-3-methoxyphenyl) fractions [51]. Due to thermal and thermocatalytic reactions, degraded products are further converted to guaiacols, polyaromatic hydrocarbons (PAHs), phenols, diols, and coke. The catalyst's efficacy can be explained by its ability to produce low molecular weight deoxygenated compounds.

3.5. Thermogravimetric Analysis

The TGA curve is used to determine the weight loss of the obtained samples during programmed thermal degradation; meanwhile, the DTG is a plot of the rate of weight loss regarding time or temperature. TGA-DTG curves of the lignin, softwood chips, and obtained bio-oils analyses were shown in Figure 6. While the degradation of wood chips and lignin samples after dehydration has occurred in only one step, the thermal degradation of the bio-oils happened in multi-steps, including dehydration, devolatilization, and decomposition of carbonaceous components stages.

Stage I of thermal degradation for wood chips and lignin pyrolysis started from room temperature to 445 and 393 K, respectively, with a slight mass loss of raw samples due to dehydration [52]. The weight loss of the bio-oils during this stage was dramatically higher than raw samples indicating the high amount of low molecular weight species in bio-oils. The surface tension tends to cause evaporation to both moisture content and the low molecular weight components. When the temperature reaches the end of stage I, the molecular forces lead to the breaking of the hydrogen bonds in the lignin and cellulose structures. When most of the moisture content in the lignin and wood chips derived bio-oils have been evaporated, the weight of the bio-oils decreases dramatically in all samples.

This indicated that the bio-oils had experienced Stage II decomposition in the temperature range from 500 to 570 K and 500 to 640 K for wood chips and lignin-based bio-oils, respectively. In this phase, bio-oil organic compound undergoes the pyrolysis process for carbon and volatile component extraction. In this stage, the transglycosylation process happens, where the cellulose chains degrade to oligosaccharides and levoglucosan [53].

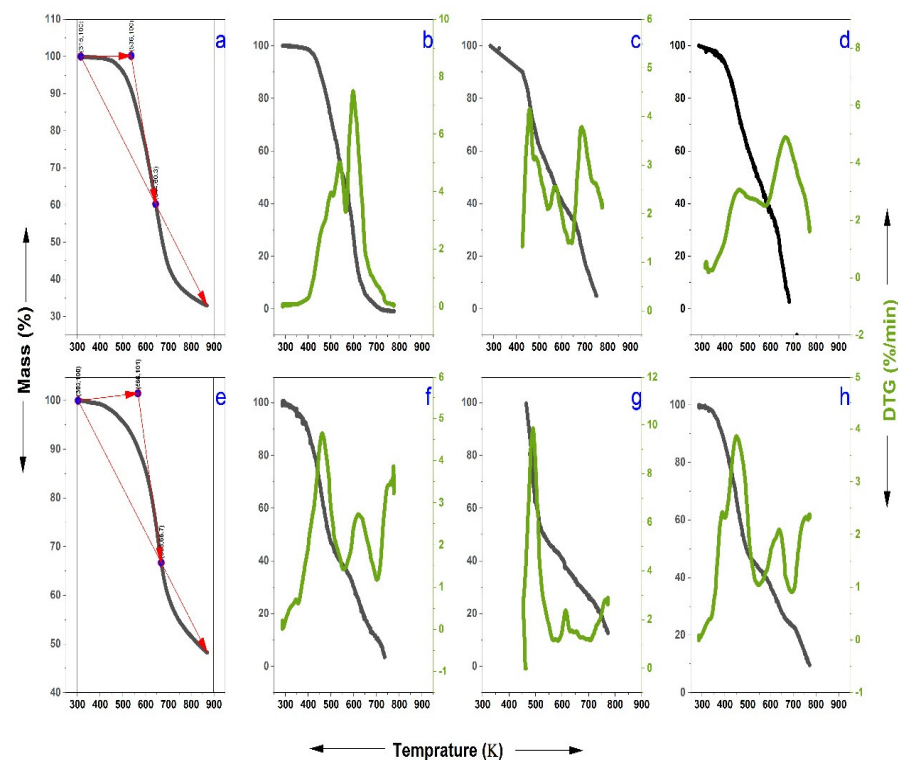


Figure 6. Thermogravimetric analysis of raw samples and obtained bio-oil: (a) Spruce wood chips; (b) bio-oil from wood chips at 673 K; (c) bio-oil from wood chips at 773 K; (d) bio-oil from wood chips at 873 K; (e) lignin sample; (f) bio-oil from lignin at 673 K; (g) bio-oil from lignin at 773 K; (h) bio-oil from lignin at 873 K.

In stage III, a slight weight loss of wood chips and lignin-based bio-oils occurs with the temperature range from 570 to 770 K and 640 to 780 K, respectively, due to the occurrence of the passive pyrolysis process. The passive pyrolysis process is where the carbonaceous component starts to decompose, and both carbon monoxide and carbon dioxide start to form by fast vaporization of non-volatile compounds in the solid residue of the biomass [54]. In addition, aromatization and cracking led to the formation of char and volatile moieties leading to the high mass loss at stage II at 400–700 K. The mass loss observed in the average range of the residual mass (%) from the onset to the endset temperature of stage II is represented in Table 9. The mass loss for softwood chips, lignin, and their obtained bio-oils in different pyrolysis temperatures in stage II was estimated to be 30–40%.

Table 9. Thermogravimetric data of raw materials and corresponding bio-oils in stage II of thermal degradation.

Sample ID	Onset Temperature (K)	Endset Temperature (K)	Max Degradation Temperature (K)	Residual Mass (%)
Lignin	445	863	668	40
Lignin-673 K	563	704	616	30
Lignin-773 K	461	562	491	37
Lignin-873 K	401	528	453	24
Softwood chips	393	864	643	33
S-wood-673 K	562	678	597	40
S-wood-773 K	426	652	459	33
S-wood-873 K	401	606	447	32

4. Conclusions

Catalytic and non-catalytic bio-oils obtained from two different biomasses have been characterized and compared to examine the effect of H-ZSM-5 as a catalyst in upgrading pyrolysis bio-oil samples. The maximum bio-oil yield has been reported for bio-oil obtained from softwood at 873 K for both catalytic and non-catalytic bio-oil samples. The physical properties of catalytic and non-catalytic bio-oil samples have been compared, and the results indicate that the main effect of H-ZSM-5 has been observed on the amount of water and oxygen for all four bio-oil samples at three different temperatures, where a significant reduction has been achieved compared to non-catalytic bio-oil samples. In addition, a significant viscosity reduction has been reported compared to non-catalytic bio-oil samples, and less viscous bio-oil samples have been obtained by catalytic pyrolysis. Furthermore, the obtained results show that the heating values have been increased for upgraded bio-oil samples compared to non-catalytic bio-oil samples. The results obtained by GCMS analysis of the catalytic bio-oil samples indicate that toluene and methanol have shown very similar behavior in the extraction of bio-oil samples compared to non-catalytic experiments. However, methanol performed a better extraction of chemicals at a higher temperature. The use of H-ZSM-5 decreased nitrogen and sulphur contents in the liquid bio-oil. However, large hydrocarbon chain compounds are absorbed in the catalyst pores or cracked into smaller chains.

For this reason, it has been observed that more compounds have been extracted by catalytic pyrolysis. H-ZSM-5 partially deoxygenated the bio-oils to aromatic hydrocarbons due to the high density of Brønsted acid sites. Compared to uncatalyzed bio-oil samples, catalysis decreased the oxygen content of the bio-oil sample by approximately 40%.

Supplementary Materials: The following supporting information can be downloaded at: <https://www.mdpi.com/article/10.3390/en16062715/s1>, Figure S1: GC-MS chromatogram resulting from H-ZSM-5 upgraded bio-oil from Kraft Lignin-Toluene Soluble: (a) 673 K; (b) 773 K and; (c) 873 K–MeOH Soluble; (d) 673 K; (e) 773 K and; (f) 873 K; Figure S2: GC-MS chromatogram resulting from H-ZSM-5 upgraded bio-oil from Spruce (Softwood) Toluene Soluble: (a) 673 K; (b) 773 K and; (c) 873 K–MeOH Soluble; (d) 673 K; (e) 773 K and; (f) 873 K.

Author Contributions: Conceptualization, A.A., Z.E.Z. and B.S.; methodology, A.A. and Z.E.Z.; software, A.A. and Z.E.Z.; validation, A.A., Z.E.Z. and B.S.; formal analysis, Z.E.Z., A.A., S.G.B. and B.S.; investigation, Z.E.Z. and A.A.; resources, Z.E.Z., A.A. and B.S.; data curation, A.A., S.G.B. and Z.E.Z.; writing—original draft preparation, A.A. and Z.E.Z.; writing—review and editing, F.S., M.M., X.Z. and B.S.; visualization, A.A., Z.E.Z. and B.S.; supervision, A.A. and B.S.; funding acquisition, B.S. All authors have read and agreed to the published version of the manuscript.

Funding: This research received no external funding.

Acknowledgments: Zahra Echresh Zadeh was partially supported by the School of Engineering, London South Bank University. The authors are thankful to the University of Tehran for supporting this work. Some figures included in the article have been adapted from the cited references.

Conflicts of Interest: The authors declare no conflict of interest.

References

1. Echresh, Z.; Abdulkhani, A.; Saha, B. A comparative structural characterisation of different lignin biomass. In Proceedings of the ECOS 2019—32nd International Conference on Efficiency, Cost, Optimization, Simulation and Environmental Impact of Energy Systems, Wrocław, Poland, 23–28 June 2019.
2. Jeong, Y.W.; Choi, S.K.; Choi, Y.S.; Kim, S.J. Production of biocrude-oil from swine manure by fast pyrolysis and analysis of its characteristics. *Renew. Energy* **2015**, *79*, 14–19. [[CrossRef](#)]
3. Zadeh, Z.E.; Abdulkhani, A.; Saha, B. Characterization of fast pyrolysis bio-oil from hardwood and softwood lignin. *Energies* **2020**, *13*, 887. [[CrossRef](#)]
4. Qambrani, N.A.; Rahman, M.M.; Won, S.; Shim, S.; Ra, C. Biochar properties and eco-friendly applications for climate change mitigation, waste management, and wastewater treatment: A review. *Renew. Sustain. Energy Rev.* **2017**, *116*, 32–46. [[CrossRef](#)]

5. Caroca, E.; Serrano, A.; Borja, R.; Jiménez, A.; Carvajal, A.; Braga, A.; Rodriguez-Gutierrez, G.; Feroso, F.G. Influence of phenols and furans released during thermal pretreatment of olive mill solid waste on its anaerobic digestion. *Waste Manag.* **2021**, *120*, 202–208. [[CrossRef](#)]
6. Xu, D.; Lin, J.; Ma, R.; Hou, J.; Sun, S.; Ma, N. Fast pyrolysis of algae model compounds for bio-oil: In-depth insights into the volatile interaction mechanisms based on DFT calculations. *Fuel* **2023**, *333*, 126449. [[CrossRef](#)]
7. Zeumer, R.; Galhano, V.; Monteiro, M.S.; Knopf, B.; Meisterjahn, B.; Amadeu, M.M.; Loureiro, S.; Lopes, I.; Schlechtriem, C. *Jo I P. Sci. Total Environ.* **2020**, *723*, 137974. [[CrossRef](#)]
8. Li, P.; Shi, X.; Jiang, L.; Wang, X.; Song, J.; Fang, S.; Bai, J.; Chang, C.; Pang, S. Synergistic enhancement of bio-oil quality through hydrochloric or acetic acid-washing pretreatment and catalytic fast pyrolysis of biomass. *Ind. Crops Prod.* **2022**, *187*, 115474. [[CrossRef](#)]
9. Li, C.; Nishu, Yellezuome, D.; Li, Y.; Liu, R.; Cai, J. Enhancing bio-aromatics yield in bio-oil from catalytic fast pyrolysis of bamboo residues over bi-metallic catalyst and reaction mechanism based on quantum computing. *Fuel* **2023**, *336*, 127158. [[CrossRef](#)]
10. Alcazar-Ruiz, A.; Dorado, F.; Sanchez-Silva, L. Bio-phenolic compounds production through fast pyrolysis: Demineralizing olive pomace pretreatments. *Food. Bioprod. Process.* **2023**, *137*, 200–213. [[CrossRef](#)]
11. Trubetskaya, A.; von Berg, L.; Johnson, R.; Moore, S.; Leahy, J.J.; Han, Y.; Lange, H.; Anca-Couce, A. Production and characterization of bio-oil from fluidized bed pyrolysis of olive stones, pinewood, and torrefied feedstock. *J. Anal. Appl. Pyrolysis* **2023**, *169*, 105841. [[CrossRef](#)]
12. Zhong, S.; Zhang, B.; Liu, C.; Aldeen, A.S.; Mwenya, S.; Zhang, H. A minireview on catalytic fast co-pyrolysis of lignocellulosic biomass for bio-oil upgrading via enhancing monocyclic aromatics. *J. Anal. Appl. Pyrolysis* **2022**, *164*, 105544. [[CrossRef](#)]
13. Gao, W.; Wan, Y.; Zhao, S.; Akhtar, M.A.; Ding, K.; Li, B.; Wu, Y.; Zhang, S.; Zhang, S. Effects of furanic compounds from biomass pyrolysis on ketonization reaction: The role of oxygenated side groups. *Fuel* **2023**, *332*, 1371–1380. [[CrossRef](#)]
14. Douvartzides, S.; Charisiou, N.D.; Wang, W.; Papadakis, V.G.; Polychronopoulou, K.; Goula, M.A. Catalytic fast pyrolysis of agricultural residues and dedicated energy crops for the production of high energy density transportation biofuels. Part II: Catalytic research, *Renew. Energy* **2022**, *189*, 315–338. [[CrossRef](#)]
15. Mendoza-Martinez, C.; Sermiyagina, E.; Saari, J.; Ramos, V.; Vakkilainen, E.; Cardoso, M.; Rocha, E.A. Fast Oxidative Pyrolysis of Eucalyptus Wood Residues to Replace Fossil Oil in Pulp Industry. *SSRN Electron. J.* **2022**, *263*, 126076. [[CrossRef](#)]
16. Hasan, M.M.; Rasul, M.G.; Jahirul, M.I.; Khan, M.M.K. Fast pyrolysis of macadamia nutshell in an auger reactor: Process optimization using response surface methodology (RSM) and oil characterization. *Fuel* **2022**, *333*, 123708. [[CrossRef](#)]
17. Li, C.; Li, Y.; Jiang, Y.; Zhang, L.; Zhang, S.; Ding, K.; Li, B.; Wang, S.; Hu, X. Staged pyrolysis of biomass to probe the evolution of fractions of bio-oil. *Energy* **2023**, *263*, 125873. [[CrossRef](#)]
18. Qing, M.; Long, Y.; Liu, L.; Yi, Y.; Li, W.; He, R.; Yin, Y.; Tian, H.; He, J.; Cheng, S.; et al. Pyrolysis of the food waste collected from catering and households under different temperatures: Assessing the evolution of char structure and bio-oil composition. *J. Anal. Appl. Pyrolysis* **2022**, *164*, 105543. [[CrossRef](#)]
19. Tran, Q.K.; Le, M.L.; Ly, H.V.; Woo, H.C.; Kim, J.; Kim, S.S. Fast pyrolysis of pitch pine biomass in a bubbling fluidized-bed reactor for bio-oil production. *J. Ind. Eng. Chem.* **2021**, *98*, 168–179. [[CrossRef](#)]
20. Taib, R.M.; Abdullah, N.; Aziz, N.S.M. Bio-oil derived from banana pseudo-stem via fast pyrolysis process. *Biomass Bioenergy* **2021**, *148*, 106034. [[CrossRef](#)]
21. Shah, M.A.; Khan, N.S.; Kumar, V.; Qurashi, A. Pyrolysis of walnut shell residues in a fixed bed reactor: Effects of process parameters, chemical and functional properties of bio-oil. *J. Environ. Chem. Eng.* **2021**, *9*, 11–13. [[CrossRef](#)]
22. Hernando, H.; Gómez-Pozuelo, G.; Botas, J.A.; Serrano, D.P. Evaluating fractional pyrolysis for bio-oil speciation into holocellulose and lignin derived compounds. *J. Anal. Appl. Pyrolysis* **2021**, *154*, 105019. [[CrossRef](#)]
23. Li, Y.; Shaheen, S.M.; Rinklebe, J.; Ma, N.L.; Yang, Y.; Ashraf, M.A.; Chen, X.; Peng, W.X. Pyrolysis of *Aesculus chinensis* Bunge Seed with Fe₂O₃/NiO as nanocatalysts for the production of bio-oil material. *J. Hazard. Mater.* **2021**, *416*, 126012. [[CrossRef](#)] [[PubMed](#)]
24. Urrutia, R.I.; Yeguerman, C.; Jesser, E.; Gutierrez, V.S.; Volpe, M.A.; González, J.O.W. Sunflower seed hulls waste as a novel source of insecticidal product: Pyrolysis bio-oil bioactivity on insect pests of stored grains and products. *J. Clean. Prod.* **2021**, *287*, 125000. [[CrossRef](#)]
25. Syazaidah, I.; Bakar, M.S.A.; Reza, M.S.; Azad, A.K. Ex-situ catalytic pyrolysis of chicken litter for bio-oil production: Experiment and characterization. *J. Environ. Manag.* **2021**, *297*, 113407. [[CrossRef](#)] [[PubMed](#)]
26. Church, A.L.; Hu, M.Z.; Lee, S.J.; Wang, H.; Liu, J. Selective adsorption removal of carbonyl molecular foulants from real fast pyrolysis bio-oils. *Biomass Bioenergy* **2020**, *136*, 105522. [[CrossRef](#)]
27. Soka, O.; Oyekola, O. A feasibility assessment of the production of char using the slow pyrolysis process. *Heliyon* **2020**, *6*, e04346. [[CrossRef](#)]
28. Kim, Y.M.; Jae, J.; Myung, S.; Sung, B.H.; Dong, J.I.; Park, Y.K. Investigation into the lignin decomposition mechanism by analysis of the pyrolysis product of *Pinus radiata*. *Bioresour. Technol.* **2016**, *219*, 371–377. [[CrossRef](#)] [[PubMed](#)]
29. Kalia, V.C.; Patel, S.K.S.; Shanmugam, R.; Lee, J.K. Polyhydroxyalkanoates: Trends and advances toward biotechnological applications. *Bioresour. Technol.* **2021**, *326*, 124737. [[CrossRef](#)] [[PubMed](#)]

30. Kumar, R.; Strezov, V.; Weldekidan, H.; He, J.; Singh, S.; Kan, T.; Dastjerdi, B. Lignocellulose biomass pyrolysis for bio-oil production: A review of biomass pre-treatment methods for production of drop-in fuels. *Renew. Sustain. Energy Rev.* **2020**, *123*, 109763. [[CrossRef](#)]
31. Zadeh, Z.E.; Abdulkhani, A.; Aboelazayem, O.; Saha, B. Recent insights into lignocellulosic biomass pyrolysis: A critical review on pretreatment, characterization, and products upgrading. *Processes* **2020**, *8*, 799. [[CrossRef](#)]
32. Saidi, M.; Samimi, F.; Karimipourfard, D.; Nimmanwudipong, T.; Gates, B.; Rahimpour, M. Upgrading of lignin-derived bio-oils by catalytic hydrodeoxygenation. *Energy Environ. Sci.* **2014**, *7*, 103–129. [[CrossRef](#)]
33. Liu, S.; Wu, G.; Gao, Y.; Li, B.; Feng, Y.; Zhou, J.; Hu, X.; Huang, Y.; Zhang, S.; Zhang, H. Understanding the catalytic upgrading of bio-oil from pine pyrolysis over CO₂-activated biochar. *Renew. Energy* **2021**, *174*, 517–535. [[CrossRef](#)]
34. Ansari, K.B.; Kamal, B.; Beg, S.; Khan, M.W.; Khan, M.S.; Al Mesfer, M.K.; Danish, M. Recent developments in investigating reaction chemistry and transport effects in biomass fast pyrolysis: A review. *Renew. Sustain. Energy Rev.* **2021**, *150*, 111454. [[CrossRef](#)]
35. Dorado, C.; Mullen, C.A.; Boateng, A.A. H-ZSM5 catalyzed co-pyrolysis of biomass and plastics. *ACS Sustain. Chem. Eng.* **2014**, *2*, 301–311. [[CrossRef](#)]
36. Tan, S.; Zhang, Z.; Sun, J.; Wang, Q. Recent progress of catalytic pyrolysis of biomass by HZSM-5. *Cuihua Xuebao/Chin. J. Catal.* **2013**, *34*, 641–650. [[CrossRef](#)]
37. Zhang, Y.; Duan, D.; Lei, H.; Villota, E.; Ruan, R. Jet fuel production from waste plastics via catalytic pyrolysis with activated carbons. *Appl. Energy* **2019**, *251*, 113337. [[CrossRef](#)]
38. Apunda, M.O.; Ogenga, D. Catalytic hydrothermal upgrading of pyrolysis oil. *Open Sci. J.* **2016**, *1*, 28–36. [[CrossRef](#)]
39. Sharma, R.K.; Bakhshi, N.N. Catalytic Upgrading of Pyrolysis Oil. *Energy Fuels* **1993**, *7*, 306–314. [[CrossRef](#)]
40. Stephanidis, S.; Nitsos, C.; Kalogiannis, K.; Iliopoulou, E.F.; Lappas, A.A.; Triantafyllidis, K.S. Catalytic upgrading of lignocellulosic biomass pyrolysis vapours: Effect of hydrothermal pre-treatment of biomass. *Catal. Today* **2011**, *167*, 37–45. [[CrossRef](#)]
41. Tursunov, O.; Kustov, L.; Tilyabaev, Z. Catalytic activity of H-ZSM-5 and Cu-HZSM-5 zeolites of medium SiO₂/Al₂O₃ ratio in conversion of n-hexane to aromatics. *J. Pet. Sci. Eng.* **2019**, *180*, 773–778. [[CrossRef](#)]
42. Zadeh, Z.E.; Abdulkhani, A.; Saha, B. A comparative production and characterisation of fast pyrolysis bio-oil from Populus and Spruce woods. *Energy* **2021**, *214*, 118930. [[CrossRef](#)]
43. Zheng, Y.; Wang, F.; Yang, X.; Huang, Y.; Liu, C.; Zheng, Z.; Gu, J. Study on aromatics production via the catalytic pyrolysis vapor upgrading of biomass using metal-loaded modified H-ZSM-5. *J. Anal. Appl. Pyrolysis* **2017**, *134*, 641–646. [[CrossRef](#)]
44. Casoni, A.I.; Hoch, P.M.; Volpe, M.A.; Gutierrez, V.S. Catalytic conversion of furfural from pyrolysis of sunflower seed hulls for producing bio-based furfuryl alcohol. *J. Clean. Prod.* **2018**, *178*, 237–246. [[CrossRef](#)]
45. Rollmann, L.D.; Walsh, D.E. Shape Selectivity and Carbon Formation in Zeolites. *J. Catal.* **1979**, *56*, 139–140. [[CrossRef](#)]
46. Csicsery, S.M. Shape-selective catalysis in zeolites. *Zeolites* **1984**, *4*, 116–126. [[CrossRef](#)]
47. Corma, A. Inorganic Solid Acids and Their Use in Acid-Catalyzed Hydrocarbon Reactions. *Chem. Rev.* **1995**, *95*, 559–614. [[CrossRef](#)]
48. Chen, N.Y.; Garwood, W.E. Industrial Application of Shape-Selective Catalysis. *Catal. Rev. Eng.* **1986**, *28*, 185–264. [[CrossRef](#)]
49. Guda, V.K.; Toghiani, H. Altering bio-oil composition by catalytic treatment of pine wood pyrolysis vapors over zeolites using an auger—Packed bed integrated reactor system. *Biofuel Res. J.* **2016**, *3*, 448–457. [[CrossRef](#)]
50. Farizul, H.K.; Amin, N.A.S.; Suhardy, D.; Azhar, S.S. Catalytic Conversion of RBD Palm Oil to Gasoline: The Effect of Silica-alumina Ratio in HZSM-5. *J. Teknol.* **2007**, *47*, 262–273. [[CrossRef](#)]
51. Dorrestijn, E.; Kranenburg, M.; Poinso, D.; Mulder, P. Lignin depolymerization in hydrogen-donor solvents. *Holzforschung* **1999**, *53*, 611–616. [[CrossRef](#)]
52. Pin, T.C.; Nascimento, V.M.; Costa, A.C.; Pu, Y.; Ragauskas, A.J.; Rabelo, S.C. Structural characterization of sugarcane lignins extracted from different protic ionic liquid pretreatments. *Renew. Energy* **2020**, *161*, 579–592. [[CrossRef](#)]
53. Abdulkhani, A.; Siahraang, M.; Zadeh, Z.E.; Hedjazi, S.; Torkameh, S.; Faezipour, M. Direct catalytic conversion of bagasse fibers to furan building blocks in organic and ionic solvents. *Biomass Convers. Biorefinery* **2021**, 1–29. [[CrossRef](#)]
54. Ha, J.M.; Hwang, K.R.; Kim, Y.M.; Jae, J.; Kim, K.H.; Lee, H.W.; Kim, J.Y.; Park, Y.K. Recent progress in the thermal and catalytic conversion of lignin. *Renew. Sustain. Energy Rev.* **2019**, *111*, 422–441. [[CrossRef](#)]

Disclaimer/Publisher’s Note: The statements, opinions and data contained in all publications are solely those of the individual author(s) and contributor(s) and not of MDPI and/or the editor(s). MDPI and/or the editor(s) disclaim responsibility for any injury to people or property resulting from any ideas, methods, instructions or products referred to in the content.